The effect of droplet breakup model for reflood experiments with a high flooding rate

Seung Hyun Yoon, Kyung Doo Kim, Kwiseok Ha*, Seung Wook Lee
Reactor System Safety Research Division, Korea Atomic Energy Research Institute,
111, Daedeok-daero 989beon-gil, Yuseong-gu, Daejeon, Republic of Korea.
**Corresponding author: ksha@kaeri.re.kr*

1. Introduction

For loss of coolant accidents, the accurate prediction for the peak cladding temperature (PCT) during a reflood phase is required. From the representative reflooding experiments such as FLECHT-SEASET (FS) [1] and RBHT [2], we recently found that the time of PCT occurred simultaneously for entire rod location with moderate and high flooding rates. The measured data showed that the significant steam mass flow was produced and cooled the entire rod with its high velocity for such cases. Since the source of steam production comes from the phase change of the droplets, we implemented the breakup process of a large droplet into the system code, SPACE, for this research.

2. Background and method

2.1. Reflood phenomena in different flooding rates

The reflood phenomena could be classified with a flooding rate, as shown in Fig. 1 [3]. In a low flooding rate, the quench front is formed at the end of the annular liquid film and generates small droplets at the downstream. In a high flooding rate, inverted annular flow (IAF) is constructed after the quench front and generates large liquid droplets at inverted slug flow (ISF) by the separation of liquid core. Eventually, these large liquid droplets will break into small droplets and contribute to the vapor generation. However, all of well-known system codes did not deal with the transient droplet breakup process.

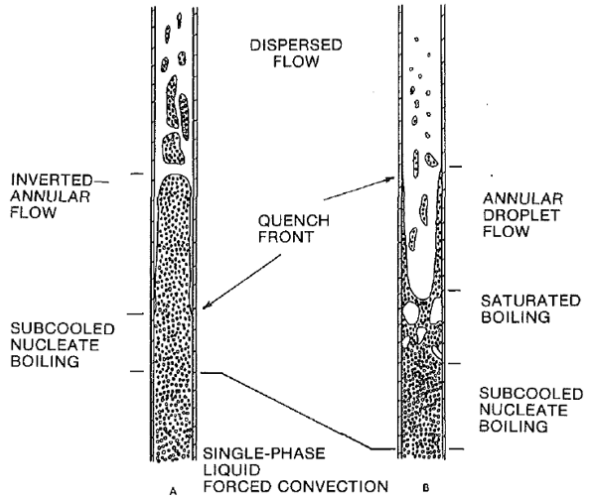

Fig. 1. The flow regimes of reflood, A : high, B : low flooding rate [3].

Fig. 2 and 3 showed that the different behavior of PCT time for rod axial locations between FS-31504 and FS-31701 experiments. The PCT times for each axial location are different for FS-31504 as 41.8 s at 1.2 m, 114.8 s at 2.0 m, 175.3 s at 3.0 m, and 272.3 s at 3.5 m. However, PCT times are almost same as 4.5 s after the reflood start for FS-31701 from 1.2 m to 3.5 m of the rod axial location.

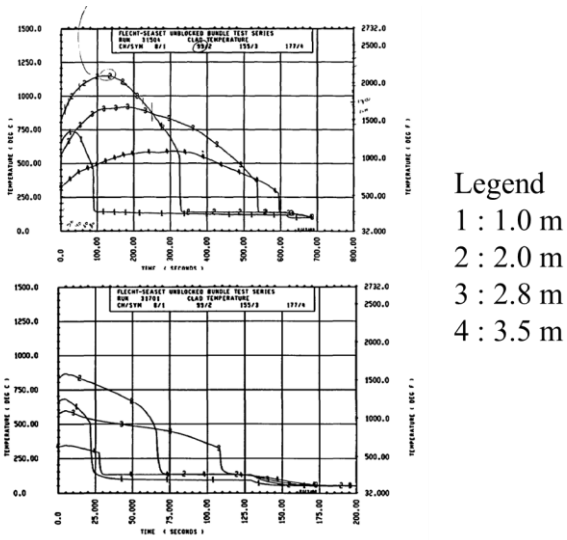

Fig. 2. Wall temperature vs. time for FS-31504 (24 mm/s) and FS-31701 (155 mm/s).

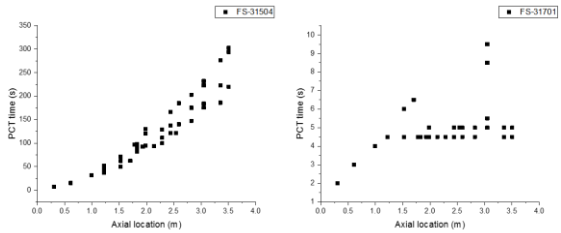

Fig. 3. PCT time vs. rod axial location for FS-31504 (24 mm/s) and FS-31701 (155 mm/s).

The steam flow rates at the outlet were measured as described in Fig. 4. From Fig. 2 to Fig. 4, we noticed the steam velocity resulted from the steam production is key parameter to PCT times. Since the steam velocity was high, the rod temperatures of FS-31701 quickly reached to PCT time, even though the position of quench front is far. The behaviors of RBHT-1407 (76 mm/s) and RBHT-1196 (152 mm/s) are also similar. By the slow steam velocity, PCT times of FS-31504 were not simultaneous over the rod.

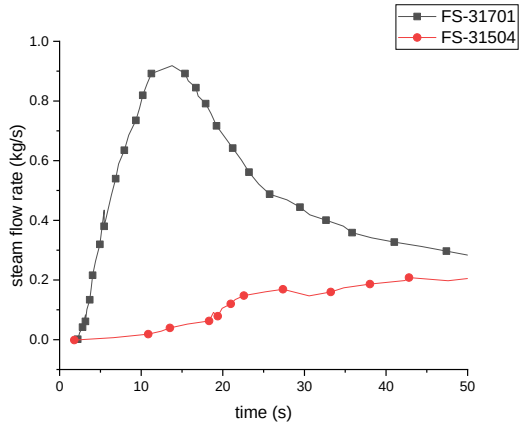

Fig. 4. Steam flow rate vs. time for FS-31504 (24 mm/s) and FS-31701 (155 mm/s).

Currently, SPACE does not predict well for the steam flow rate at the outlet. By implementing the large droplet breakup processes at ISF, we expected to increase the entrained mass of small droplets. This will lead to the more vaporization during the reflood and the realistic steam flow rate at the outlet.

2.2. Droplet breakup model

Lee and No [4] suggested a series of the equations for the droplet breakup which are applicable to the 1-D calculation. For the droplet breakup model, the Reitz-Diwakar model [5] was used as the equations (1) and (2).

$$\frac{dD}{dt} = -\frac{D - D_{stable}}{\tau} \quad (1)$$

$$D_{stable} = \begin{cases} \dfrac{\sigma^2}{\rho_g (v_g - v_D)^3 \mu_g} & \text{for stripping} \\ We_{critical} \dfrac{\sigma}{\rho_g (v_g - v_D)^2} & \text{for bag} \end{cases} \quad (2)$$

where D is a large droplet, D_{stable} is the size of a stable droplet, and τ is the lifetime of an unstable droplet. We calculated the change of the droplet size with the distance between a face and a cell or a cell and a face.

For the drag coefficient to calculate the large droplet velocity, the Shiller–Naumann model [6] was applied as the equation (3).

$$C_D = \frac{24}{\mathrm{Re}_D}(1 + 0.15\,\mathrm{Re}_D^{0.687}) \quad (3)$$

Since the droplet is moving with its velocity, the large droplet diameter of a cell should be determined with the mass-averaged value, considering mass inlet and outlet as the following equation.

$$D_{cell,1} = \frac{m_{cell,in} D_{in} + (m_{cell,0} - m_{cell,out}) D_{cell,0}}{m_{cell,in} + m_{cell,0} - m_{cell,out}} \quad (4)$$

where m means the mass, subscript 0 and 1 indicate the state for the previous time and the current time, respectively. To obtain the entrained mass at the cell, we used the mass source from the large droplet breakup as follows:

$$m_d = \rho_D \pi \frac{(D_{in})^3 - (D_{out})^3}{6} \quad (5)$$

d is a small droplet, and $m_{D,in}$ is the mass inlet for the large droplet from the face.

One should notice that the entrainment model for the reflooding core is already in SPACE. However, the breakup mechanism described in this paper is different with the entrainment model for the reflooding core. So the equation (5) and the entrainment model for the reflooding core are applied simultaneously for the code calculation.

We determined the size of the small droplet through the following equation:

$$d = \frac{1.5\sigma_d}{\rho_g (v_g - v_d)^2} \quad (6)$$

3. The effect with droplet breakup model with FS-31701

3.1. Validating experiment

FLECHT-SEASET is rod bundle experiments for reflood phenomena. The axial length of the rod bundle is 3.66 m. Here we selected FS-31701 which have operating conditions for the flooding rate of 155 mm/s, the pressure of 0.28 MPa, and the subcooling of water of 80 K. The nodalization of SPACE is described as Fig. 5.

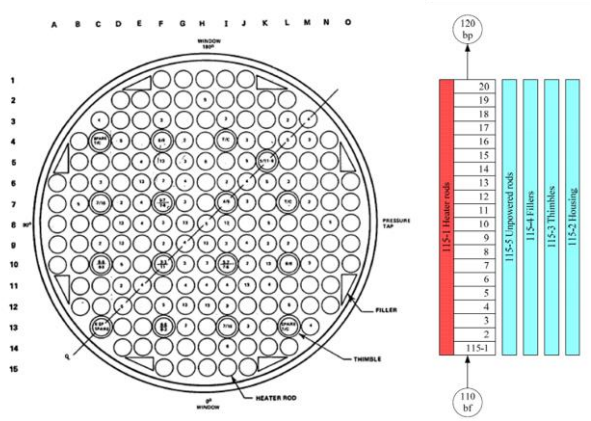

Fig. 5. Cross-section and SPACE nodalization for FLECHT-SEASET [1].

3.2. Results

In this section, we compared the steam mass flow rate at outlet, the wall temperature, and the vapor temperature at each axial locations. As shown in Fig. 6, the steam mass flow rate with the transient droplet breakup model showed better agreement than that without breakup model. By this effect, with the breakup model, we obtained the results that PCT time is even faster than the experimental one along the rod. Fig. 10 clearly showed the different PCT time.

Fig. 7 showed the modified one well followed the experimental wall temperature at 2 ft. However, as plotted in Fig. 9, the case with the breakup model showed a delayed quenching time. This may be caused by the late quenching at 4 ft, as shown in Fig. 8.

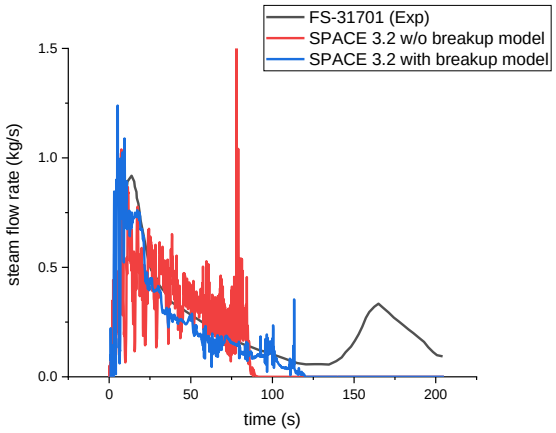

Fig. 6. Steam mass flow rate vs. time at the outlet.

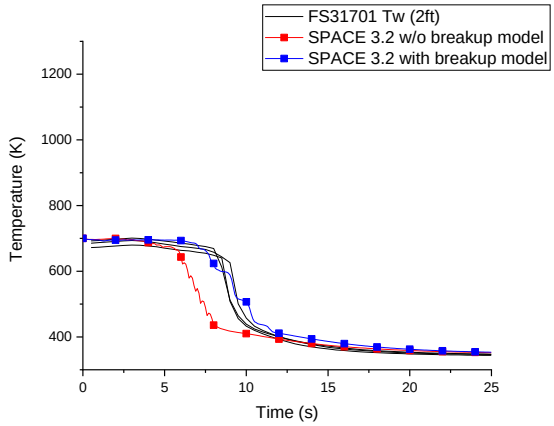

Fig. 7. Wall temperature vs. time at the rod (2 ft).

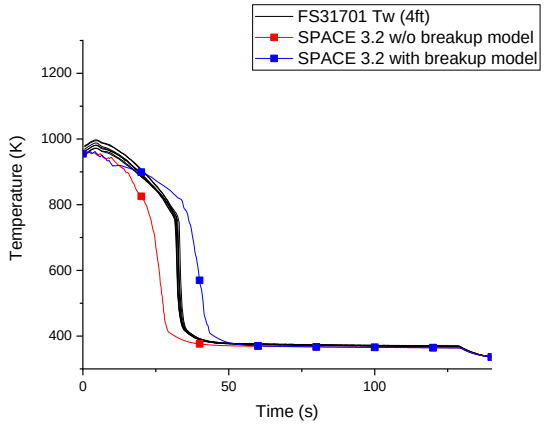

Fig. 8. Wall temperature vs. time at the rod (4 ft).

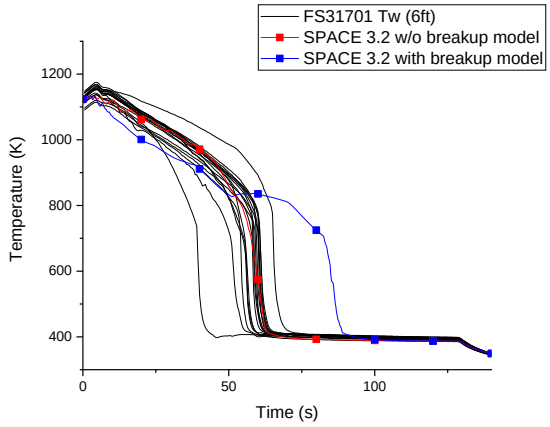

Fig. 9. Wall temperature vs. time at the rod (6 ft).

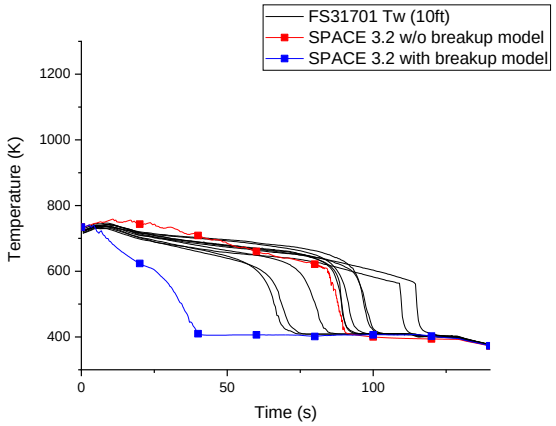

Fig. 10. Wall temperature vs. time at the rod (10 ft).

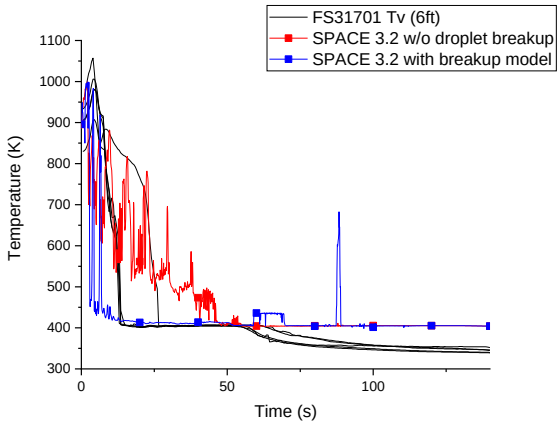

Fig. 11. Vapor temperature vs. time at the rod (6 ft).

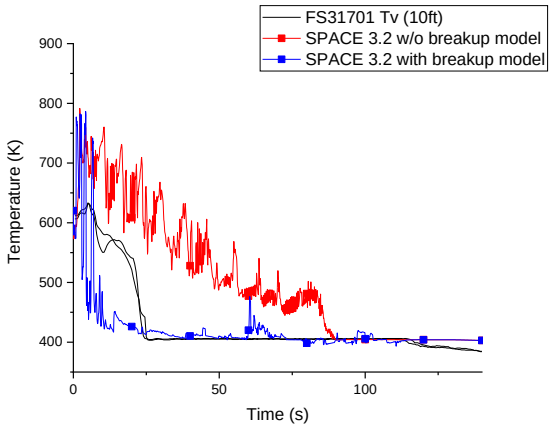

Fig. 12. Vapor temperature vs. time at the rod (10 ft).

As observed in Fig. 10, the wall temperature with the breakup model showed fast temperature decrease at the film boiling regime before the quench. This can be resulted from the rapid decrease of the vapor temperature, as shown in Fig. 12. Since the vapor generation is large with the breakup model, the vapor temperature decreases faster with the breakup model than that without the breakup model. The rapid drop of vapor temperature cause high heat transfer from the wall to the vapor by its large temperature difference. To resolve this high heat transfer, more study on the vapor temperature will be required as further works.

4. Conclusions

To deliver the accurate hydraulic behavior, this study focused on the implementation of the transient breakup model into the system code. As a result, the outlet steam mass flow rate showed good agreements with the experiment. From this steam mass flow rate, PCT time occurred earlier than that of the original code. However, the wall temperature results from 6 ft to the top showed some deviations with the experimental results. These deviations may come from the rapid drop of the vapor temperature caused by a large vapor generation. More investigations will be mandatory to solve this remaining problem.

Acknowledgement

This work was supported and funded by Korea Hydro & Nuclear Power Co., LTD.

REFERENCES

1. N. Lee, S. Wong, H. Yeh, and L. Hochreiter, "PWR FLECHT SEASET unblocked bundle, forced and gravity reflood task data report," Electric Power Research Institute, EPRI. NUREG/CR-2256, 1981.
2. Hochreiter, L. E., F. B. Cheung, T. F. Lin, S. Ergun, A. Sridharan, A. Ireland, and E. R. Rosal. "RBHT reflood heat transfer experiments data and analysis." Tech. Rep. (2012).
3. M. Kawaji, Y. S. Ng, S. Banerjee, and G. Yadigaroglu, “Reflooding With Steady and Oscillatory Injection: Part I?Flow Regimes, Void Fraction, and Heat Transfer,” J. Heat Transfer, vol. 107, no. 3, p. 670, 2009.
4. Lee, S. W. & No, H. C. Droplet size prediction model based on the upper limit log-normal distribution function in venturi scrubber. Nucl. Eng. Technol. (2019). doi:10.1016/J.NET.2019.03.014
5. Reitz, R. D. & Diwakar, R. Structure of High-Pressure Fuel Sprays. SAE Tech. Pap. Ser. 1, 492–509 (2010).
6. Schiller, L., Naumann, Z.: A Drag Coefficient Correlation, Z. Ver. Deutsch. Ing., 77-318 (1935)